Heliyon 9 (2023) e18671

Contents lists available at ScienceDirect

Heliyon

journal homepage: www.cell.com/heliyon

# Efficient extraction of data from intra-operative evoked potentials: 1.-Theory and simulations

Mark M. Stecker [a,*], Jonathan Wermelinger [b], Jay Shils [c]

[a] Fresno Institute of Neuroscience, USA
[b] Neurosurgery Department, Inselspital, University Hospital Bern, Switzerland
[c] Department of Neurosurgery, Rush College of Medicine, USA

ARTICLE INFO

*Keywords:*
Evoked potential
Amplitude
Least squares
Correlation
Receiver
Latency
Detection

ABSTRACT

Quickly and efficiently extracting evoked potential information from noise is critical to the clinical practice of intraoperative neurophysiologic monitoring (IONM). Currently this is primarily done using trained professionals to interpret averaged waveforms. The purpose of this paper is to evaluate and compare multiple means of electronically extracting simple to understand evoked potential characteristics with minimum averaging. A number of evoked potential models are studied and their performance evaluated as a function of the signal to noise level in simulations.

*Methods:* which extract the least number of parameters from the data are least sensitive to the effects of noise and are easiest to interpret. The simplest model uses the baseline evoked potential and the correlation receiver to provide an amplitude measure. Amplitude measures extracted using the correlation receiver show superior performance to those based on peak to peak amplitude measures. In addition, measures of change in latency or shape of the evoked potential can be extracted using the derivative of the baseline evoked response or other methods. This methodology allows real-time access to amplitude measures that can be understood by the entire OR staff as they are small, dimensionless numbers of order unity which are simple to interpret. The IONM team can then adjust averaging and other parameters to allow for visual interpretation of waveforms as appropriate.

## 1. Introduction

In intra-operative neurophysiologic monitoring (IONM), evoked potentials are recorded after stimuli are delivered to different pathways and an alert is generated when there is a significant change in the response. This provides a warning about impending injury in the specific neural pathways being monitored. One problem with this paradigm is that the output of a clinical evoked potential test is a complex set of waveforms that in current clinical application requires interpretation by trained technologists and neurophysiologists even though most clinical applications are based on only amplitude and latency measurements. Another problem is that intra-operative evoked potentials are often contaminated by high amplitude electrical and biological noise [1–5]which complicates interpretation. In the clinical setting, the three primary techniques used to reduce the effect of noise include averaging [6], filtering [7] and optimization of recording parameters [8]. Averaging requires time that reduces the speed of interpretations and can yield

* Corresponding author. 1968 S. Coast Hwy Suite 550 Laguna Beach CA 926511, USA. Tel./Fax: 516-478-8304.
*E-mail address:* mark@finsneuro.org (M.M. Stecker).

https://doi.org/10.1016/j.heliyon.2023.e18671
Received 16 April 2023; Received in revised form 14 July 2023; Accepted 25 July 2023
Available online 28 July 2023

inaccurate results when the evoked potentials change rapidly. Filtering distorts the signal and is most helpful only when the frequencies contained in the evoked potential are different from those of the noise. On the other hand, optimizing recording parameters is always helpful, but even under optimal conditions it is impossible to remove all noise.

The field of signal processing has developed many ways to detect a signal in noise [9] and to find relationships between two signals in noise [10]. The classical detection method, based upon radar and sonar, uses a quadratic cost function to compare an incoming signal to an expected signal. Mathematically, this results in the "correlation receiver" where the correlation between the expected and actual signal is the measure of signal amplitude. This approach works well when the shape of the expected signal is known, such as in radar, but is not optimal when there is little knowledge of the expected signal.

In many clinical applications other than IONM, the shape of the evoked potential and/or the noise is unknown and much work has been focused on that problem [11–13]. In this particular case, there are three techniques used to extract signal from noise. If the spectrum of the noise and the signal are known, the noise can be filtered using Wiener filtering [14–16], but this is most useful when the noise and evoked potential spectra don't overlap. When the noise satisfies and autoregressive model, this can also be used to reduce the noise level [17]. It is also possible to project data into subspaces expected to be associated with less noise before analysis using independent components analysis [18] or the singular value decomposition [19]. When data from multiple locations are available, spatial filtering can be used [20]. In a related technique single trial ep data over time can be extracted from noise by creating 2-D images of stacks of single traces [21–23] and then applying image processing techniques. This can find the similarities between traces and help eliminate noise but it is not a realtime procedure as it needs to process multiple traces.

However, in IONM, the baseline studies provide the shape of the waveforms that will be encountered during the procedure. This significant advantage makes the problem of extracting information from intra-operative evoked potentials very different from that of blind waveform detection as described in the previous paragraph. Relatively little has been written on this particular problem in the IONM literature. The purpose of this paper will be to propose, simulate and evaluate automated procedures that might be able to extract information, especially amplitude, from an evoked potential during a surgical procedure when the baseline is known.

Since many different methods have been discussed in literature but rarely compared, an additional goal of this paper is to use variational approaches to set a consistent mathematical approach which allows comparison of the underpinnings of the different methods. This also facilitates comparison of the different methods both mathematically and through simulations. Some of the methodological differences in the literature focus on the roles of different cost functions and the use of a priori information through constraints. These differences are discussed in detail to facilitate future searches for optimal methods.

## 2. Methods

### 2.1. Annotation

$x(T)$ will be used to denote a continuous measurement of a signal at time T recorded from a patient exposed to n stimuli delivered at times $\tau_i; i = 1...n$. Each evoked potential is recorded for a time $t_{\max}$ after each stimulus. The capital T will be used to denote times from the start of the surgery and the small t (or q) will denote the time after the latest stimulus. $s_i(t)$ will be used as the actual evoked response recorded at time t after a stimulus at time 0. As such, the evoked response $s_i(t)$ must begin only after the stimulus so $s_i(t) = 0, t < t_a$ where $t_a$ is the shortest time after the stimulus at which an evoked potential can be recorded. It will also be assumed that the evoked response has a finite duration so $s_i(t) = 0, t > t_s$ with $t_s$ shorter than any inter-stimulus interval (i.e. $0 < t_a < t_s < t_{\max} < Min[\{\tau_{i+1} - \tau_i\}]; i = 1...n-1$) as in Figure A7. In other words, each of the responses is assumed to have a finite support: shorter in duration than the shortest time between stimuli and shorter than the length of the recording after each stimulus.

$s(t)$ will be used to denote the evoked response to the stimuli in the absence of noise in the steady state where the response is to each stimulus is the same from trial to trial. In a situation where the actual $s(t)$ is not known a priori, this can represent a "trial function" or guess as to a reasonable choice for the actual response. Within this framework, $x(T)$ is the sum of the actual evoked response from each trial and noise for each time point:

$$x(T) = \sum_{i=1}^{n} s_i(T - \tau_i) + N(T) \tag{1}$$

To distinguish the estimated value of the evoked potential from the (unknown) actual response, the estimated responses will be denoted as $\widehat{s}_i(t)$. A cost function will be used to compare two signals and will generally be denoted by I. The studies in the body of this paper use the $L_2$ or quadratic cost function. In appendix (A.2) other cost functions are studied and results compared.

To put the evoked potential signal detection algorithms in perspective, it is useful to consider a number of scenarios classified according to the a priori assumptions made. Section 2.2 discusses models in which no assumptions are made about a specific shape for $s_i(t)$ and section 2.3 treats models in which the shape of $s_i(t)$ is not arbitrary but determined by a few parameters. Appendix A.4 will address the situation in which $s_i(t)$ can take on only two distinct values and how this can be used to classify cases.

### 2.2. Models where the shape of the response is unknown

#### 2.2.1. Steady state with minimal trial to trial variation

In the steady state $s_i(t) = s(t)$ and so the least squares estimate of the evoked potential $s(t)$ results from minimizing (0.2):

$$I[\widehat{s}\,] = \sum_{i=1}^{n} \int_{0}^{t_{\max}} dt \left| x(t+\tau_i) - \sum_{i=1}^{n} \widehat{s}\,(t) \right|^2 \tag{2}$$

where I is the least squares difference between the actual and the proposed evoked potential.

Minimizing I with respect to $\widehat{s}$ results in the solution (0.3):

$$\frac{\partial I[\widehat{s}\,]}{\partial \widehat{s}\,(q)} = 0 \rightarrow \frac{1}{n} \sum_{i=1}^{n} [x(q+\tau_i)] = \widehat{s}\,(q); 0 \le q \le t_{\max} \tag{3}$$

This estimate is exactly the traditional averaging procedure that is applied to evoked potential recordings and illustrates that traditional averaging gives the least squares best estimate of the evoked potential in the steady state when there is no a priori knowledge of the shape of the response, except that it is stable from trace to trace. In IONM, the assumption is made that the responses are in a steady state for the periods of time while each average is collected.

It is important to note that this result depends on using the least squares $L_2$ metric for the cost of poor fit between the actual and proposed signal. Other cost functions, particularly the $L_1$ which measures the absolute value of the difference between the values of the signals, can be used although they are computationally more difficult. Appendix A.2 presents more information on this issue and demonstrates that, in this case, for large values of n, the $L_1$ and $L_2$ cost functions give the similar results. However, for small values of n, the result that the mean over all traces is the best predictor is seen only with the $L_2$ cost function. For this reason and the computational simplicity, most of this study will involve the $L_2$ cost function.

It is useful to quantitate the effect of noise on the estimated response. Substituting equation (0.1) into (0.3) yields (0.4):

$$\begin{aligned} &\frac{1}{n} \sum_{i=1}^{n} x(q+\tau_i) = \widehat{s}\,(q) = s(q) + \widetilde{s}(q) \\ &\frac{1}{n} \sum_{i=1}^{n} N(q+\tau_i) = \widetilde{s}(q) \end{aligned} \tag{4}$$

where $\widetilde{s}(t)$ represents the effect of noise. In the case where the noise has zero mean (See appendix A.1 for more details about handling the situation in which the data and trial function do not have zero mean.), then if a large number of experiments were performed and the averages taken (denoted by the angle brackets $\langle\rangle$) (0.5):

$$\begin{aligned} &\langle \widetilde{s}(q) \rangle = 0 \\ &\sqrt{\langle \widetilde{s}(q)^2 \rangle} = \frac{\sqrt{\left\langle \left( \sum_{i=1}^{n} N(q+\tau_i) \right)^2 \right\rangle}}{n} \end{aligned} \tag{5}$$

If the noise is further assumed to be stationary and uncorrelated between different stimuli:

$$\langle N(q+\tau_i) N(q+\tau_j) \rangle = \begin{Bmatrix} i = j, \langle N(q) N(q) \rangle \\ i \ne j, 0 \end{Bmatrix}$$

then the result is (0.6):

$$\sqrt{\left\langle \widetilde{s}(q)^2 \right\rangle} = \frac{\sqrt{\left\langle \left( \sum_{i=1}^{n} N(q+\tau_i) \right)^2 \right\rangle}}{n} = \frac{\sqrt{\left\langle (N(q))^2 \right\rangle}}{\sqrt{n}} \tag{6}$$

Hence as expected the effect of noise in the estimation of the evoked response diminishes as the inverse of the square root of the number of averages.

### 2.2.2. Trace to trace variations allowed

In many situations the assumption that the evoked responses do not vary from trial to trial is not a good one. In this case, the least squares determination of the evoked potential comes from minimizing the least squares cost (0.7):

$$\begin{aligned} &I[\{\widehat{s}_i\}] = I[\widehat{s}\,] = \sum_{i=1}^{n} \int_{0}^{t_{\max}} dt \left| x(t+\tau_i) - \sum_{i=1}^{n} \widehat{s}_i(t) \right|^2 \\ &\frac{\partial I[\{\widehat{s}_i\}]}{\partial \widehat{s}_i(q)} = 0 \rightarrow x(q+\tau_i) = \widehat{s}_i(q); 0 \le q \le t_{\max} \end{aligned} \tag{7}$$

Intuitively, when nothing is known about the trace to trace variability of the responses, the only choice is to take the evoked

responses as equal to the recorded signal. Thus, the cost of making no assumptions (such as the assumption of steady state) is that the algorithm has no way of telling signal from noise. In this case (still assuming the noise to be stationary and uncorrelated), the noise level in the responses is determined from (0.8):

$$\begin{aligned}&\langle \widetilde{s}_i(q)\rangle = 0\\ &\sqrt{\langle \widetilde{s}_i(q)^2\rangle} = \sqrt{\langle (N(q))^2\rangle}\end{aligned} \tag{8}$$

which differs from (0.6) by the factor $\frac{1}{\sqrt{n}}$ . Thus, the price of not making the steady state assumption is that the noise level in each estimated evoked potential is much larger than if the steady state assumption were made. This is consistent with the idea that the increasing the amount of accurate a priori information about the evoked response, lowers the effect of noise on the estimated potential.

### 2.2.3. *The shape of the evoked response is unknown but constrained*

In this case, the cost function has the form (0.9):

$$I[\{\widehat{s}_i\}] = \sum_{i=1}^{n}\int_0^{t_{\max}} dt\left|x(t+\tau_i) - \sum_{i=1}^{n}\widehat{s}_i(t)\right|^2 + \xi\sum_{i=2}^{n}\int_0^{t_{\max}} dt\left|s_i^0(t) - \widehat{s}_i(t)\right|^2 \tag{9}$$

where $s_i^0(t)$ is presumed to be known a priori. This results in the solution (0.10):

$$\begin{aligned}&\frac{\partial I[\{\widehat{s}_i\}]}{\partial \widehat{s}_i(q)} = 0 \rightarrow (x(q+\tau_i) - \widehat{s}_i(q)_i) + \xi\left(s_i^0(q) - \widehat{s}_i(q)\right) = 0\\ &\frac{x(q+\tau_i) + \xi s_i^0(q)}{1+\xi} = \widehat{s}_i(q); 0 < q \le t_{\max}\end{aligned} \tag{10}$$

## 2.3. *Parametric models*

The above methods have assumed that relatively little is known about the expected shape of the evoked potential from trial to trial $s_i(t)$. However, in IONM, there is quite a bit known about the form of the evoked potential recorded from a set of electrodes in response to a standardized stimulus [24]. Thus, another set of models might be based on the assumption that during an OR case, all important variations in the evoked potential from trial to trial can be described by changes in a few parameters describing an evoked response such as amplitude, latency and duration [12,25,26].

A general, parametric representation of the recorded data is (0.11):

$$x(T) \rightarrow \sum_{i=1}^{n} a_i\sigma\left(T-\tau_i, \left\{P_i^{(k)}\right\}\right) + N(T) \tag{11}$$

where $\sigma(t, \{P_i^{(k)}\}); 0 \le t \le t_{\max}$ can be any function of t that depends on the $n_p$ parameters $\{P_i^{(1)} \ldots P_i^{(n_p)}\}$ which may vary from trace to trace. $a_i$ is the amplitude index for each trace. All of the variations in the shape of the response from trace to trace are contained in the changes in the parameters $\{P_i^{(k)}\}$ . One simple choice is to take $\sigma(T-\tau_i, \{P_1^{(k)}\}) = s(t)$, the **known** "steady state" baseline response, but many other choices would be possible. The function $\sigma(t, \{P_i^{(k)}\})$ will be referred to as the "trial function". In this approach, no averaging is specified and the variations from trial to trial can be estimated.

In general, the values of all unknown parameters can be estimated through a least-squares method with the cost function (0.12):

$$I\left(\{\widehat{a}_i\}, \left\{\widehat{P}_i^{(k)}\right\}\right) = \sum_{i=1}^{n}\int_0^{t_{\max}} dt\left|x(t+\tau_i) - \sum_{i=1}^{n}\widehat{a}_i\sigma\left(t, \left\{\widehat{P}_i^{(k)}\right\}\right)\right|^2 \tag{12}$$

Although the parameters may enter into the cost function in complex ways, the amplitude measures have a simple effect on the cost function and so it is easy to determine the amplitudes that minimize the cost function (0.13):

$$\frac{\partial I\left(\{\widehat{a}_i\}, \left\{\widehat{P}_i^{(k)}\right\}\right)}{\partial \widehat{a}_i} = 0 \rightarrow \widehat{a}_i = \frac{\int_0^{t_{\max}} dt x(t+\tau_i)\sigma\left(t, \left\{\widehat{P}_i^{(k)}\right\}\right)}{\int_0^{t_{\max}} dt\sigma\left(t, \left\{\widehat{P}_i^{(k)}\right\}\right)^2} \tag{13}$$

This leads to a cost estimate as a function of the parameters $\{P_i^{(k)}\}$ as (0.14):

$$I(\{\widehat{P}_i^{(k)}\}) = \sum_{i=1}^{n} \int_0^{t_{\max}} dt x(t+\tau_i)^2 - \sum_{i=1}^{n} \frac{\left( \int_0^{t_{\max}} dt x(t+\tau_i)\sigma(t, \{\widehat{P}_i^{(k)}\}) \right)^2}{\int_0^{t_{\max}} dt \sigma(t, \{\widehat{P}_i^{(k)}\})^2} \tag{14}$$

thus, estimating the amplitude is relatively simple while finding the values of the $\{P_i^{(k)}\}$ that control the shape of the trial function and minimize $I(\{\widehat{P}_i^{(k)}\})$ is much more complex and is highly dependent on the choice of the trial function.

### 2.3.1. Trace to trace variations described by changes in amplitude, latency and duration

The most intuitive trial function would be the steady state baseline evoked potential, s(t), which could be shifted in latency or duration (or more properly "time warping") (0.15):

$$\sigma(t, \{\widehat{P}_i^{(k)}\}) = s(\widehat{w}_i(t - \widehat{\varphi}_i)) \tag{15}$$

This fits in well with visual analysis where changes from the baseline shape are monitored. However, not all possible choices for $\widehat{w}_i, \widehat{\varphi}_i$ yield acceptable trial functions. The requirement that the response to a stimulus must be delayed from the stimulus onset any chosen parameters forces $\sigma(t, \{\widehat{P}_i^{(k)}\}) = 0; t \le t_a$. The fact that the evoked potential does not have a longer duration than the recording window implies that $\sigma(t, \{\widehat{P}_i^{(k)}\}) = 0; t \ge t_{\max}$. These are satisfied if (0.16):

$$\begin{aligned} &\widehat{w}_i(t_a - \widehat{\varphi}_i) \ge t_a \rightarrow (\widehat{w}_i - 1)t_a \ge \widehat{w}_i\widehat{\varphi}_i \\ &\widehat{w}_i(t_{\max} - \widehat{\varphi}_i) \le t_{\max} \rightarrow (\widehat{w}_i - 1)t_{\max} \le \widehat{w}_i\widehat{\varphi}_i \end{aligned} \tag{16}$$

in addition, it is expected that intra-operative damage would be associated with increased latencies $\varphi_i > 0$ and increased durations $w_i \le 1$. Now (0.17):

$$\int_0^{t_{\max}} dt \sigma(t, \{\widehat{P}_i^{(k)}\})^2 = \int_0^{t_{\max}} dt s(w_i(t - \varphi_i))^2 = \frac{1}{w_i} \int_{-w_i\varphi_i}^{w_i(t_{\max} - \varphi_i)} dt' s(t')^2 \tag{17}$$

when $-w_i\varphi_i \le t_a; w_i(t_{\max} - \varphi_i) \ge t_s$ this simplifies to (0.18):

$$\begin{aligned} &\int_0^{t_{\max}} dt \sigma(t, \{\widehat{P}_i^{(k)}\})^2 = \frac{S}{w_i} \\ &S = \int_0^{t_{\max}} dt s(t')^2 \end{aligned} \tag{18}$$

Under these simplifying conditions, the criteria for minimizing $I(\{\widehat{P}_i^{(k)}\}) = I(\{\widehat{\varphi}_i, \widehat{w}_i\})$ become (0.19):

$$\begin{aligned} &I(\{\widehat{\varphi}_i, \widehat{w}_i\}) = \sum_{i=1}^{n} \int_0^{t_{\max}} dt x(t+\tau_i)^2 + \frac{1}{S} \sum_{i=1}^{n} w_i \left( \int_0^{t_{\max}} dt x(t+\tau_i) s(\widehat{w}_i(t - \widehat{\varphi}_i)) \right)^2 \\ &\frac{\partial I(\{\widehat{\varphi}_i, \widehat{w}_i\})}{\partial \widehat{\varphi}_i} = 0 \rightarrow \int_0^{t_{\max}} dt x(t+\tau_i) s'(\widehat{w}_i(t - \widehat{\varphi}_i)) = 0 \\ &\frac{\partial I(\{\widehat{\varphi}_i, \widehat{w}_i\})}{\partial \widehat{w}_i} = 0 \rightarrow \widehat{w}_i = -\frac{\int_0^{t_{\max}} dt x(t+\tau_i) s(\widehat{w}_i(t - \widehat{\varphi}_i))}{2 \int_0^{t_{\max}} dt x(t+\tau_i)(t - \widehat{\varphi}_i) s'(\widehat{w}_i(t - \widehat{\varphi}_i))} \end{aligned} \tag{19}$$

As a check, it is relatively simple to show if s is continuous that these equations yield the expected result $\widehat{\varphi}_i = 0, \widehat{w}_i = 1$ when $x(t + \tau_i) = s(t)$. Appendix A.4 shows that the trial function may not have the expected intuitive meaning unless $-w_i\varphi_i \le 0; w_i(t_{\max} - \varphi_i) \ge t_s$. Of course, all positive latency shifts with $\widehat{w}_i = 1$ do satisfy this criterion. However, even in this case, solving these equations can be complex and so it is useful to consider some special cases.

*2.3.1.1. Changes in the evoked potential from trial to trial can be described mainly by changes in amplitude.* The simplest case is when it is presumed that the waveform changes only in amplitude over the course of the study. In this case $\varphi_i = 0, w_i = 1$ and so (0.13) becomes (0.20):

$$\widehat{a}_i = \frac{\int_0^{t_{max}} dt\ x(t+\tau_i)s(t)}{\int_0^{t_{max}} dt\ s(t)^2} \tag{20}$$

This is the classical "correlation receiver" and provides the best estimate of the single trial evoked potential amplitude in this model relative to the baseline. Note, that if the evoked potential experiment was in the steady state without noise, then: $\int_0^{t_{max}} dt\ x(t+\tau_i)s(t) = \int_0^{t_{max}} dt\ s(t)^2$ and so $\widehat{a}_i = 1$ as expected.

It is important to see how this amplitude estimate is affected by noise. As above, let: $x(T) = \sum_{i=1}^{n} a_i s(T-\tau_i) + N(T)$.
so that (0.21):

$$\begin{aligned} \widehat{a}_i &= a_i + \frac{\int_0^{t_{max}} dt\ N(t+\tau_i)s(t)}{\int_0^{t_{max}} dt\ s(t)^2} \\ \langle \widehat{a}_i \rangle &= a_i \\ \left\langle (\widehat{a}_i - a_i)^2 \right\rangle &= \frac{\left\langle \int_0^{t_{max}} dt\ N(t+\tau_i)s(t) \int_0^{t_{max}} dt'\ N(t'+\tau_i)s(t') \right\rangle}{S^2} \end{aligned} \tag{21}$$

If the autocorrelation function of the noise is known (0.22):

$$\begin{aligned} &\langle N(t)N(t') \rangle = \nu g(t-t'); g(-t) = g(t); g(0) = 1 \\ &G = \int_{-\infty}^{\infty} dt g(t) \end{aligned} \tag{22}$$

Then (0.23):

$$\left\langle (\widehat{a}_i - a_i)^2 \right\rangle = \frac{\left\langle \int_0^{t_{max}} dt\ N(t+\tau_i)s(t) \int_0^{t_{max}} dt'\ N(t'+\tau_i)s(t') \right\rangle}{S^2} = \frac{\nu \int_0^{t_{max}} \int_0^{t_{max}} dt dt'\ g(t-t')s(t)s(t')}{S^2} \tag{0.23}$$

If the noise autocorrelation is significant different from 0 only over time periods so short that s(t) does not vary significantly (i.e. the noise is nearly white), it is possible to write (0.24):

$$V_a^2 = \left\langle (\widehat{a}_i - a_i)^2 \right\rangle \approx \frac{\nu G}{S} \tag{24}$$

This is just the total noise power divided by the total power in the trial function (i.e. signal). It is important to notice that this decreases as the duration of the template signal increases.

For comparison, it is useful to compute the peak to peak amplitude $A_i^{pp}$ of the putative evoked potential after each stimulus and its variability once the peak and trough times for the signal $t_{peak}, t_{trough}$ are known:

$$\begin{aligned} A_i^{pp} &= s(t_{peak}) + N(t_{peak}+\tau_i) - s(t_{trough}) - N(t_{trough}+\tau_i) \\ \langle A_i^{pp} \rangle &= s(t_{peak}) - s(t_{trough}) \\ \left\langle (A_i^{pp} - \langle A_i^{pp} \rangle)^2 \right\rangle &= 2\nu g(0); \left| g(t_{peak} - t_{trough}) \right| \ll g(0) \\ V_{pp}^2 &= \frac{\left\langle (A_i^{pp} - \langle A_i^{pp} \rangle)^2 \right\rangle}{\langle A_i^{pp} \rangle^2} = \frac{2\nu g(0)}{\left( s(t_{peak}) - s(t_{trough}) \right)^2} \end{aligned}$$

now $\frac{V_a^2}{V_{pp}^2}$ is an index of the effects of noise on the two different amplitude indices (0.25):

$$\frac{V_a^2}{V_{pp}^2} = \frac{G}{2g(0)} \frac{\left(s\left(t_{peak}\right) - s\left(t_{trough}\right)\right)^2}{S} \tag{25}$$

Notice that this is independent of the actual amplitude of the noise or signal and is only dependent on their shapes. Defining (0.26):

$$\begin{aligned} D_s &= \frac{\int_{-\infty}^{\infty} dt s(t)^2}{\left(s\left(t_{peak}\right) - s\left(t_{trough}\right)\right)^2} \\ D_N &= \frac{\int_{-\infty}^{\infty} dt g(t)}{g(0)} \end{aligned} \tag{26}$$

These are markers of the duration of the signal s and time over which correlations in the noise are significant respectively. In terms of these variables (0.27):

$$\frac{V_a^2}{V_{pp}^2} = \frac{G}{2g(0)} \frac{\left(s\left(t_{peak}\right) - s\left(t_{trough}\right)\right)^2}{S} = \frac{1}{2} \frac{D_N}{D_S} \tag{27}$$

Thus, the ratio of noise estimates from the correlation receiver and the peak to peak measurement increases as the duration of the trial function increases and as the time over which the noise is autocorrelated is decreased. In fact, with discretely sampled signals with white noise, $D_N$ approaches 1 and $D_s$ approaches the number of sample points over which the signal has significant power and hence $\sqrt{\frac{V_a^2}{V_{pp}^2}}$ diminishes as $\frac{1}{\sqrt{n_s}}$ where $n_s$ is the number of sample points over which s(t) is non-zero. This is as expected since, with the correlation receiver, the amplitude is the result of averaging the noise over the time periods where the signal has high amplitude. This emphasizes that the estimates of the amplitude can be improved using the correlation receiver by increasing the sample rate up to the point where it reaches at least the inverse of the correlation time of the noise. In this model, the optimum sample rate is not simply that which defines the signal but it must also fully define the noise.

One important question is what the role of the choice of cost function in this context is. Appendix A2.2 shows that both the $L_1$ and $L_2$ cost functions can be used to extract a reasonable estimate of the actual amplitude of the evoked potential while other cost functions do not provide as good results. The standard deviation of the estimates using the $L_1$ cost function as in Figure S4 are higher than with the $L_2$ cost function.

*2.3.1.2. Amplitude estimations when only an approximate steady-state response is known.* The above approach used knowledge of the form of the evoked response to be detected $s(t)$. It is useful to explore the case in which instead of $s(t)$, there is knowledge only of an approximate signal $s_a(t) \neq s(t)$. In the case where $x(T) = \sum_{i=1}^{n} a_i s(T - \tau_i)$, (0.13) becomes (0.28):

$$\widehat{a}_i = a_i \frac{\int_0^{t_{\max}} dt \; s(t) s_a(t)}{\int_0^{t_{\max}} dt \; s_a(t)^2} \tag{28}$$

As long as the two signals are correlated $\left| \int_0^{t_{\max}} dt \; s(t) s_a(t) \right| > 0$, then, although the amplitude estimates may not be accurate, relative variations over time are still accurate. In order to understand this from a more practical level, it is useful to explore the simple case in which both s and $s_a$ are rectangular functions having amplitudes of A and $A_a$ and widths of r and $r_a$ respectively. Then (0.29):

$$\widehat{a}_i = a_i \frac{\int_0^{t_{\max}} dt \; s(t) s_a(t)}{\int_0^{t_{\max}} dt \; s_a(t)^2} = a_i \frac{A}{A_a} \frac{Min[r, r_a]}{r_a} \tag{29}$$

Thus, when the duration of the approximate template is shorter than that of the actual signal $r > r_a$ the estimated amplitude from the least squares method is directly proportional to the exact amplitude and does not vary with the actual choice of $r_a$ or $r$. However, if $r < r_a$, the amplitude estimate will decrease as $r_a$ increases. This shows that, under many circumstances, reasonable choices of the

evoked potential template yield amplitude measures proportional to the actual amplitude and hence could be used in evoked potential monitoring. Appendix section A3 shows more general results.

*2.3.1.3. Effects of data transformation on amplitude estimates.* Many previous investigations involving extracting single trace evoked potentials [11,17,27] have focused on means of reducing the effect of noise. In particular, it is commonly proposed that certain types of "noise" (especially that from cerebral activity) may be well fit by an autoregressive model. In such cases, it is possible to apply the corresponding "whitening filter" to the data and the evoked potential template. Because this results in white noise, as noted above, the parameter estimates will have less variability. It is useful to note that even if the signal is transformed before analysis as long as the template signal is transformed similarly, the resulting amplitude estimate from the correlation receiver is the same. Consider these linear transformations of the template and data (0.30):

$$
\begin{aligned}
&s_c(t) = \int_0^{t_{\max}} c(t,t')s(t')dt' \\
&x_c(t+\tau_i) = \int_0^{t_{\max}} c(t,t')x(t'+\tau_i)dt' \\
&a_c = \frac{\int_0^{t_{\max}} dt\ x_c(t+\tau_i)s_c(t)}{\int_0^{t_{\max}} dt\ s_c(t)^2} = \frac{\int_0^{t_{\max}} dtdt'dt''c(t,t')c(t,t'')\ x(t''+\tau_i)s(t')}{\int_0^{t_{\max}} dt\,dt'dt''c(t,t')c(t,t'')s(t')s(t'')} = \frac{\int_0^{t_{\max}} dt'dt''d(t',t'')\ x(t''+\tau_i)s(t')}{\int_0^{t_{\max}} dt'dt''d(t',t'')s(t')s(t'')} \\
&d(t',t'') = \int_0^{t_{\max}} c(t,t')c(t,t'')dt \\
&x(T) \rightarrow \sum_{i=1}^{n} a_i s(T-\tau_i) + N(T) \\
&a_{ci} = a_i + \frac{\int_0^{t_{\max}} dt'dt''d(t',t'')\ N(t''+\tau_i)s(t')}{\int_0^{t_{\max}} dt'dt''d(t',t'')s(t')s(t'')} \\
&\langle a_{ci}\rangle = a_i \\
&\left\langle (a_{ci}-a_i)^2 \right\rangle = \left\langle \left( \frac{\int_0^{t_{\max}} dt'dt''d(t',t'')\ N(t''+\tau_i)s(t')}{\int_0^{t_{\max}} dt'dt''d(t',t'')s(t')s(t'')} \right)^2 \right\rangle = \frac{\nu \int_0^{t_{\max}} dt'dt''dt'''dt''''d(t',t'')d(t''',t'''')\ g(t''-t''')s(t')s(t''')}{\left( \int_0^{t_{\max}} dt'dt''d(t',t'')s(t')s(t'') \right)^2}
\end{aligned}
\tag{30}
$$

Thus, transforming both the signal and template gives us the same estimate of amplitude on average (when the trial function is a multiple of the actual evoked potential) but the effect of noise can be different depending on how c is chosen. Section 2.2.3.1 shows that the variance is as low as possible when the correlation function of the noise has the shortest duration. If there is a single type of noise obeying a single model, such a transformation can be of value but if there are multiple noise sources, this can be problematic as a transformation which "whitens" or shortens the correlation time for one noise source can increase the correlation time of other noise sources.

*2.3.1.4. Effect of latency and duration variations on the correlation receiver amplitude measure.* The latency and duration of the evoked potential may also vary over time. The purpose of this section is to understand how those variations might affect the amplitude produced from the correlation receiver if these variations were not specifically corrected for.

$$\widehat{a}_i = \frac{\int_0^{t_{max}} dt\ x(t+\tau_i)s(t)}{\int_0^{t_{max}} dt\ s(t)^2}$$

If $x(t+\tau_i) = a_0 s(t+\varphi)$ for some small value of $\varphi$ a series expansion can be used (0.31):

$$\widehat{a}_i = a_0 \frac{\int_0^{t_{max}} dt\ s(t+\varphi)s(t)}{\int_0^{t_{max}} dt\ s(t)^2} \approx a_0 + \varphi a_0 \frac{\int_0^{t_{max}} dt\ s'(t)s(t)}{\int_0^{t_{max}} dt\ s(t)^2} + \frac{1}{2}\varphi^2 a_0 \frac{\int_0^{t_{max}} dt\ s''(t)s(t)}{\int_0^{t_{max}} dt\ s(t)^2} + \ldots$$

$$\int_0^{t_{max}} dt\ s'(t)s(t) = 0; \int_0^{t_{max}} dt\ s''(t)s(t) = -\int_0^{t_{max}} dt\ s'(t)^2 \tag{31}$$

$$\widehat{a}_i = a_0 \left(1 - \frac{1}{2}\varphi^2 \frac{\int_0^{t_{max}} dt\ s'(t)^2}{\int_0^{t_{max}} dt\ s(t)^2}\right)$$

So, if no explicit correction is made for latency shifts, the amplitude estimated from the correlation receiver would undergo an apparent reduction in amplitude for small latency shifts. Thus, declines in amplitude could be due to an actual change in amplitude or a change in latency but the latter effects are very small for small changes in latency as the effect is proportional to $\varphi^2$.

In the same way, the effect of a small change in the duration (w) of the signal on measured amplitude of the signal can be computed (0.32):

$$\widehat{a}_i = \frac{\int_0^{t_{max}} dt\ s(wt)s(t)}{\int_0^{t_{max}} dt\ s(t)^2}; w = 1+\omega; \omega \ll 1$$

$$\int_0^{t_{max}} dt\ s((1+\omega)t)s(t) \approx \int_0^{t_{max}} dt\ s(t)s(t) + \omega \int_0^{t_{max}} dt\ ts'(t)s(t) + \frac{1}{2}\omega^2 \int_0^{t_{max}} dt\ t^2 s''(t)s(t) + \ldots$$

$$\int_0^{t_{max}} dt\ t^2 s''(t)s(t) = \int_0^{t_{max}} dt\, s(t)^2 - \int_0^{t_{max}} dt\, t^2 s'(t)^2$$

$$\int_0^{t_{max}} dt\ s((1+\omega)t)s(t) \approx \int_0^{t_{max}} dt\ s(t)s(t) - \frac{\omega}{2}\int_0^{t_{max}} dt\, s(t)^2 + \frac{1}{2}\omega^2 \left[\int_0^{t_{max}} dt\, s(t)^2 - \int_0^{t_{max}} dt\, t^2 s'(t)^2\right] + \ldots \tag{32}$$

$$= \int_0^{t_{max}} dt\ s(t)s(t) \left(1 - \frac{\omega}{2} + \frac{1}{2}\omega^2 \left[1 - \frac{\int_0^{t_{max}} dt\, t^2 s'(t)^2}{\int_0^{t_{max}} dt\ s(t)s(t)}\right]\right)$$

$$\widehat{a} = a_0 \left(1 - \frac{\omega}{2} + \frac{1}{2}\omega^2 \left[1 - \frac{\int_0^{t_{max}} dt\, t^2 s'(t)^2}{\int_0^{t_{max}} dt\ s(t)s(t)}\right]\right)$$

This fits with the bound placed by the Cauchy-Schwartz inequality (0.33):

$$\frac{\left(\int_0^{t_{\max}} dt\ \ s(wt)s(t)\right)^2}{\int_0^{t_{\max}} dt\, s(t)^2 \int_0^{t_{\max}} dt\, s(wt)^2} \leq 1 \rightarrow \frac{\left|\int_0^{t_{\max}} dt\ \ s(wt)s(t)\right|}{\int_0^{t_{\max}} dt\, s(t)^2} \leq \frac{1}{\sqrt{w}} \tag{33}$$

Given that small changes in duration near $w_i = 1$ cause linear changes in the amplitude estimate while small changes in latency near $\varphi_i = 0$ are associated with second order changes, it is expected that slight changes in duration may have larger effects on the amplitude estimated by the correlation receiver. In addition, even small reductions in w (longer durations) can cause increased amplitude measurements and so interpretation of the correlation receiver response would require some measure describing the change in shape of the response. It is rare in the clinical situation for amplitude, latency and duration shifts to occur independently and so a better estimate of the effect of shape changes on the correlation receiver amplitude can be estimated only if we know the likely trajectory of changes in $w_i$ and $\varphi_i$ during IONM.

*2.3.1.5. Least squares determination of latency shifts.* The equation determining the latency (0.19) does not involve the amplitude and so the latency can be determined independently. Basically, the latency is determined by shifting s to maximize the overlap between s(t) and the recorded signal. This is, in general, a better way to determine the latency than a formal solution of the equations but for small latency shifts (0.19) yields (0.34):

$$\begin{aligned} &\int_0^{t_{\max}} dt\, x(t+\tau_i)s'(t-\widehat{\varphi}_i) = 0 \rightarrow \int_0^{t_{\max}} dt\, x(t+\tau_i)s'(t) - \widehat{\varphi}_i \int_0^{t_{\max}} dt\, x(t+\tau_i)s''(t) = 0 \\ &\widehat{\varphi}_i \approx \frac{\int_0^{t_{\max}} dt\, x(t+\tau_i)s'(t)}{\int_0^{t_{\max}} dt\, x(t+\tau_i)s''(t)} \end{aligned} \tag{34}$$

This reveals one of the problems in estimating the latency using the least squares approach. The calculated change in latency is heavily dependent on higher order derivatives of the expected signal and hence may be unreliable in the presence of noise.

A rough estimate of the effect of noise on the estimation of latency can be made when:

$$x(T) = \sum_{i=1}^{n} s(T-\tau_i) + N(T)$$

as (0.35):

$$\begin{aligned} &\widehat{\varphi} \approx \frac{\int_0^{t_{\max}} dt[s(t)+N(t+\tau_i)]s'(t)}{\int_0^{t_{\max}} dt\,[s(t)+N(t+\tau_i)]s''(t)} \approx \frac{\int_0^{t_{\max}} dt[N(t+\tau_i)]s'(t)}{\int_0^{t_{\max}} dt\,[s(t)]s''(t)}; \left|\int_0^{t_{\max}} dt\,[s(t)]s''(t)\right| \gg \left|\int_0^{t_{\max}} dt\,[N(t+\tau_i)]s''(t)\right| \\ &\int_0^{t_{\max}} dts(t)s'(t) = 0 \rightarrow \langle\varphi\rangle = 0 \\ &s(t)s''(t) = \frac{d}{dt}[s(t)s'(t)] - s'(t)^2 \rightarrow \int_0^{t_{\max}} dt\,[s(t)]s''(t) = -\int_0^{t_{\max}} dt\, s'(t)^2 = -S' \\ &\langle\widehat{\varphi}^2\rangle \approx \frac{\nu G \int_0^{t_{\max}} dts'(t)^2}{\left(\int_0^{t_{\max}} dt\, s'(t)^2\right)^2} = \frac{\nu G}{S'} \end{aligned} \tag{35}$$

where it has been assumed that the signal to noise ratio is high. This has a similar form to that of the estimate for the variance in the amplitude estimate except that the denominator relates to the derivative of the expected signal. Again, this variance decreases as the duration of the signal increases but it also decreases for signals with higher derivatives or sharper contours. This is to be expected since it is easier to align signals with sharp contours. In the case where the noise is very high in amplitude compared to the signal the

assumption in (0.35) is not valid and (0.36):

$$\widehat{\varphi} \approx \frac{\int_0^{t_{\max}} dt[s(t)+N(t+\tau_i)]s^{'}(t)}{\int_0^{t_{\max}} dt\,[s(t)+N(t+\tau_i)]s^{''}(t)} \approx \frac{\int_0^{t_{\max}} dt[N(t+\tau_i)]s^{'}(t)}{\int_0^{t_{\max}} dt\,[N(t+\tau_i)]s^{''}(t)}; \left|\int_0^{t_{\max}} dt\,[s(t)]s^{''}(t)\right| \ll \left|\int_0^{t_{\max}} dt\,[N(t+\tau_i)]s^{''}(t)\right|$$

$$\int_0^{t_{\max}} dts(t)s^{'}(t) = 0 \rightarrow \langle\varphi\rangle = 0$$

$$s(t)s^{''}(t) = \frac{d}{dt}[s(t)s^{'}(t)] - s^{'}(t)^2 \rightarrow \int_0^{t_{\max}} dt\,[s(t)]s^{''}(t) = -\int_0^{t_{\max}} dt\,s^{'}(t)^2 = -S^{'} \tag{36}$$

$$\langle\widehat{\varphi}^{\,2}\rangle \approx \frac{\nu G\int_0^{t_{\max}} dts^{'}(t)^2}{\left(\int_0^{t_{\max}} dt\,s^{'}(t)^2\right)^2} = \frac{\nu G}{S^{'}}$$

If the noise is sinusoidal then (0.37):

$$N(t+\tau_i) = A\,\mathrm{Sin}(\omega t)$$

$$\widehat{\varphi} \approx \frac{\int_0^{t_{\max}} dt[s(t)+N(t+\tau_i)]s^{'}(t)}{\int_0^{t_{\max}} dt\,[s(t)+N(t+\tau_i)]s^{''}(t)} \approx \frac{\int_0^{t_{\max}} dt\,\mathrm{Sin}(\omega t)s^{'}(t)}{\int_0^{t_{\max}} dt\,\mathrm{Sin}(\omega t)s^{''}(t)}$$

$$\int_0^{t_{\max}} dt\,\mathrm{Sin}(\omega t)s^{''}(t) = \omega\int_0^{t_{\max}} dt\,\mathrm{Cos}(\omega t)s^{''}(t); s^{'}(0) = 0, s^{'}(t_{\max}) = 0 \tag{37}$$

$$\widehat{\varphi} \approx \frac{\int_0^{t_{\max}} dt\,\mathrm{Sin}(\omega t)s^{'}(t)}{\omega\int_0^{t_{\max}} dt\,\mathrm{Cos}(\omega t)s^{'}(t)}$$

So that in this case the noise induced latency shift is inversely proportional to the frequency of the noise.

### 2.3.2. Other trial functions

*2.3.2.1. Derivatives of the steady state response.* Although the latency and duration trial function has intuitive appeal, it is complex and the parameters are not truly independent (A4). Other trial functions can provide a better index for shape changes. One very simple choice is (0.38):

$$x(T) \rightarrow \sum_{i=1}^{n} a_i s(T-\tau_i) + \sum_{i=1}^{n} b_i s^{'}(T-\tau_i) + N(T)$$

$$I(\{\widehat{a}_{\,i}\},\{\widehat{b}_{\,i}\}) = \sum_{i=1}^{n}\int_0^{t_{\max}} dt\left|x(t+\tau_i) - \sum_{i=1}^{n}\widehat{a}_{\,i}s(t) - \sum_{i=1}^{n}\widehat{b}_{\,i}s^{'}(t)\right|^2$$

$$\frac{\partial I(\{\widehat{a}_{\,i}\},\{\widehat{b}_{\,i}\})}{\partial\widehat{a}_{\,i}} = 0 \rightarrow \int_0^{t_{\max}} dt(x(t+\tau_i) - \widehat{a}_{\,i}s(t) - \widehat{b}_{\,i}s^{'}(t))s(t) = 0 \tag{38}$$

$$\frac{\partial I(\{\widehat{a}_{\,i}\},\{\widehat{b}_{\,i}\})}{\partial\widehat{b}_{\,i}} = 0 \rightarrow \int_0^{t_{\max}} dt(x(t+\tau_i) - \widehat{a}_{\,i}s(t) - \widehat{b}_{\,i}s^{'}(t))s^{'}(t) = 0$$

Since (0.39):

$$\int_0^{t_{\max}} dts(t)s^{'}(t) = \frac{1}{2}\left(s(t_{\max})^2 - s(0)^2\right) = 0 \tag{39}$$

It is easy to show that (0.40):

$$a_i = \frac{\int_0^{t_{\max}} dtx(t+\tau_i)s(t)}{\int_0^{t_{\max}} dts(t)^2}$$
$$b_i = \frac{\int_0^{t_{\max}} dtx(t+\tau_i)s^{'}(t)}{\int_0^{t_{\max}} dts^{'}(t)^2} \tag{40}$$

Two observations are important. First, if there is no change in the shape then $b_i = 0$. Second, for small latency or duration shifts (0.41):

$$x(t+\tau_i) = s(t-\varphi) = s(t) - \varphi s^{'}(t) + \frac{1}{2}\varphi^2 s^{''}(t) + \frac{1}{6}\varphi^3 s^{'''}(t)$$
$$b_i = \frac{\int_0^{t_{\max}} dtx(t+\tau_i)s^{'}(t)}{\int_0^{t_{\max}} dts^{'}(t)^2} = -\varphi + \frac{1}{2}\varphi^2\frac{\int_0^{t_{\max}} dts^{''}(t)s^{'}(t)}{\int_0^{t_{\max}} dts^{'}(t)^2} + \frac{1}{6}\varphi^3\frac{\int_0^{t_{\max}} dts^{'''}(t)s^{'}(t)}{\int_0^{t_{\max}} dts^{'}(t)^2} + \ldots = -\varphi - \frac{1}{6}\varphi^3\frac{\int_0^{t_{\max}} dts^{''}(t)^2}{\int_0^{t_{\max}} dts^{'}(t)^2} + \ldots$$
$$x(t+\tau_i) = s((1+\omega)t) = s(t) - \omega t s^{'}(t) + \frac{1}{2}(\omega t)^2 s^{''}(t) + \frac{1}{6}(\omega t)^3 s^{'''}(t) \tag{41}$$
$$b_i = \frac{\int_0^{t_{\max}} dtx(t+\tau_i)s^{'}(t)}{\int_0^{t_{\max}} dts^{'}(t)^2} = -\omega\frac{\int_0^{t_{\max}} dt\, ts^{'}(t)^2}{\int_0^{t_{\max}} dts^{'}(t)^2} + \frac{1}{2}\omega^2\frac{\int_0^{t_{\max}} dt\, t^2 s^{''}(t)s^{'}(t)}{\int_0^{t_{\max}} dts^{'}(t)^2} + \frac{1}{6}\omega^3\frac{\int_0^{t_{\max}} dt\, t^3 s^{'''}(t)s^{'}(t)}{\int_0^{t_{\max}} dts^{'}(t)^2} + \ldots$$

So that $b_i$ is equal to the latency shift and is directly proportional to the duration shift. However, if the duration and phase co-vary, $b_i$ will not always change to lowest order if $\varphi + \omega\frac{\int_0^{t_{\max}} dt\, ts^{'}(t)^2}{\int_0^{t_{\max}} dts^{'}(t)^2} = 0$ . In the special case where the steady state evoked potential can be described as a Gaussian:

$$s(t) = Ae^{-\frac{1}{2\rho^2}(t-t_0)^2}; \frac{t_0}{\rho} \gg 1, \frac{(t_{\max} - t_0)}{\rho} \gg 1$$
$$x(t+\tau_i) = s(w(t-\varphi))$$

Then (0.42):

$$b = w2^{\frac{3}{2}}\frac{((w-1)t_0 - \varphi w)e^{-\frac{((w-1)t_0-\varphi w)^2}{2(1+w^2)\rho^2}}}{\left(1+w^2\right)^{\frac{3}{2}}}$$
$$\frac{b}{a} = \frac{2w(w-1)t_0 - 2\varphi w^2}{1+w^2} \tag{42}$$

Which is $-\varphi$ to lowest order when w = 1 as expected. It should be noted that b is zero as long as: $((w-1)t_0 - \varphi w) = 0$. Thus, this

method cannot detect all shape changes.

Using the previous discussions for the amplitude noise (equation (0.21) to (0.24)), the effect of noise on b is (0.43):

$$V_b^2 = \frac{\left\langle (\widehat{b}_i - b_i)^2 \right\rangle}{b_i^2} = \frac{\nu G}{\int_0^{t_{max}} dt s'(t)^2} = V_a^2 \frac{\int_0^{t_{max}} dt s(t)^2}{\int_0^{t_{max}} dt s'(t)^2} \tag{43}$$

For a signal discretely sampled at times $t_k, k = 1 \ldots npt$ the relation: $\int_0^{t_{max}} dt s(t) s'(t) = 0$ is replaced by (0.44):

$$\sum_{k=1}^{npt-1} (s(t_{k+1}) + s(t_k))(s(t_{k+1}) - s(t_k)) = 0 \tag{44}$$

and so, the quantities of interest are (0.45):

$$a_i = \frac{\sum_{k=1}^{npt-1} (x(t_{k+1} + \tau_i) + x(t_k + \tau_i))(s(t_{k+1}) + s(t_{ki}))}{\sum_{k=1}^{npt-1} (s(t_{k+1}) + s(t_{ki}))^2}$$
$$b_i = \frac{\sum_{k=1}^{npt-1} (x(t_{k+1} + \tau_i) + x(t_k + \tau_i))(s(t_{k+1}) - s(t_{ki}))}{\sum_{k=1}^{npt-1} (s(t_{k+1}) - s(t_{ki}))^2} \tag{45}$$

The ratio b/a and the individual values of a and b are easily computed and are still a useful index of shape change. Figures A8 and A9 compare the ability of different techniques to detect phase changes.

Appendix A5 gives additional information on the use of using correlations with the derivative of the steady state response to indicate and illustrate in a simple manner how evoked potential shape changes could affect the amplitude measure.

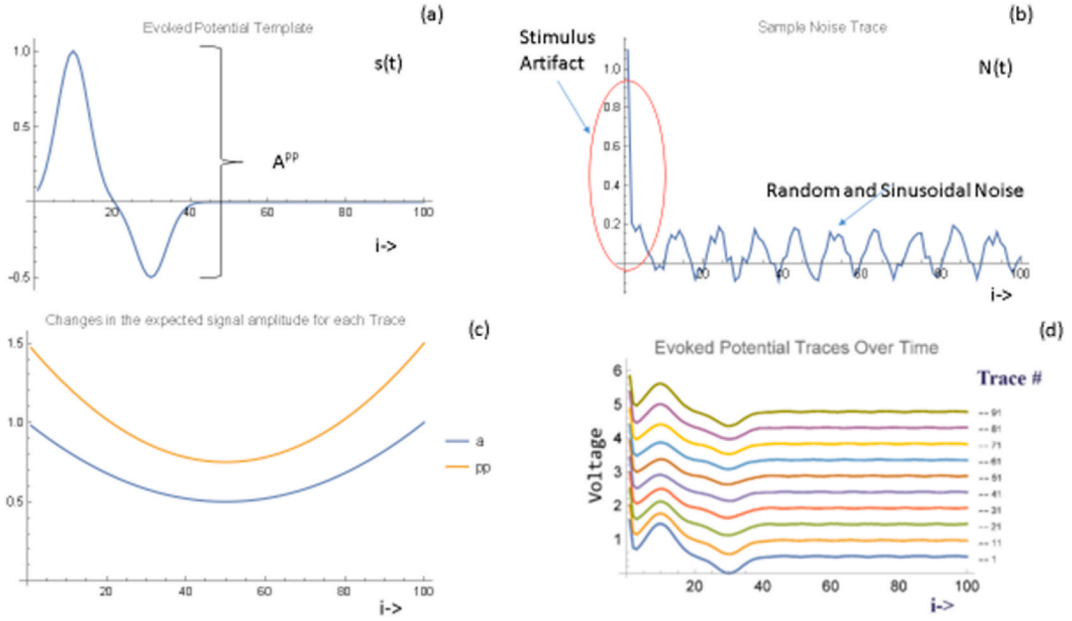


**Fig. 1.** Components of the simulation study. (a) The template for the evoked potential which is essentially the baseline response. (b) an illustration of the noise used in the simulations. (c) The planned changes in the evoked potential amplitude, a, or peak to peak amplitude, pp, over time during a given case. (d) a stacked plot showing the evoked potentials during a simulated case in the absence of noise.

*2.3.2.2. Two fixed latencies.* It is useful to explore the effects that other trial functions might have in understanding the shape and amplitude of the evoked potential. A very simple one would involve a linear mixture of the baseline response plus the baseline response shifted by a fixed amount $\varphi_i$ (0.46):

$$x(T) \rightarrow \sum_{i=1}^{n} a_i s(T-\tau_i) + \sum_{i=1}^{n} b_i s(T-\tau_i-\varphi_i) + N(T)$$

$$I(\{\widehat{a}_i\},\{\widehat{b}_i\}) = \sum_{i=1}^{n} \int_0^{t_{\max}} dt \left| x(t+\tau_i) - \sum_{i=1}^{n} \widehat{a}_i s(t) - \sum_{i=1}^{n} \widehat{b}_i s(t-\varphi_i) \right|^2$$

$$\frac{\partial I(\{\widehat{a}_i\},\{\widehat{b}_i\})}{\partial \widehat{a}_i} = 0 \rightarrow \int_0^{t_{\max}} dt(x(t+\tau_i) - \widehat{a}_i s(t) - \widehat{b}_i s(t-\varphi_i))s(t) = 0$$

$$\frac{\partial I(\{\widehat{a}_i\},\{\widehat{b}_i\})}{\partial \widehat{b}_i} = 0 \rightarrow \int_0^{t_{\max}} dt(x(t+\tau_i) - \widehat{a}_i s(t) - \widehat{b}_i s(t-\varphi_i))s(t-\varphi_i) = 0$$

$$M = \begin{bmatrix} \int_0^{t_{\max}} dt s(t)^2 & \int_0^{t_{\max}} dt s(t)s(t-\varphi_i) \\ \int_0^{t_{\max}} dt s(t)s(t-\varphi_i) & \int_0^{t_{\max}} dt s(t-\varphi_i)^2 \end{bmatrix}$$

$$S = \begin{bmatrix} \int_0^{t_{\max}} dt s(t)x(t+\tau_i) \\ \int_0^{t_{\max}} dt s(t-\varphi_i)x(t+\tau_i) \end{bmatrix} \tag{46}$$

$$\begin{bmatrix} \widehat{a}_i \\ \widehat{b}_i \end{bmatrix} = M^{-1}S = \frac{1}{\int_0^{t_{\max}} dt s(t-\varphi_i)^2 \int_0^{t_{\max}} dt s(t)^2} \frac{1}{1 - \frac{\left(\int_0^{t_{\max}} dt s(t)s(t-\varphi_i)\right)^2}{\int_0^{t_{\max}} dt s(t-\varphi_i)^2 \int_0^{t_{\max}} dt s(t)^2}} \begin{bmatrix} \int_0^{t_{\max}} dt s(t-\varphi_i)^2 & -\int_0^{t_{\max}} dt s(t)s(t-\varphi_i) \\ -\int_0^{t_{\max}} dt s(t)s(t-\varphi_i) & \int_0^{t_{\max}} dt s(t)^2 \end{bmatrix}$$

$$\begin{bmatrix} \int_0^{t_{\max}} dt s(t)x(t+\tau_i) \\ \int_0^{t_{\max}} dt s(t-\varphi_i)x(t+\tau_i) \end{bmatrix}$$

Clearly (0.47):

$$\begin{bmatrix} \widehat{a}_i \\ \widehat{b}_i \end{bmatrix} = \begin{bmatrix} 1 \\ 0 \end{bmatrix}; x(t+\tau_i) = s(t); \frac{\left(\int_0^{t_{\max}} dt s(t)s(t-\varphi_i)\right)^2}{\int_0^{t_{\max}} dt s(t-\varphi_i)^2 \int_0^{t_{\max}} dt s(t)^2} \ll 1$$

$$\begin{bmatrix} \widehat{a}_i \\ \widehat{b}_i \end{bmatrix} = \begin{bmatrix} 0 \\ 1 \end{bmatrix}; x(t+\tau_i) = s(t-\varphi_i); \frac{\left(\int_0^{t_{\max}} dt s(t)s(t-\varphi_i)\right)^2}{\int_0^{t_{\max}} dt s(t-\varphi_i)^2 \int_0^{t_{\max}} dt s(t)^2} \ll 1 \tag{47}$$

So that the deviation of $b_i$ from zero is a measure of the actual shape of the evoked response differing from s(t). Figures A8 and A9 compare the ability of different techniques to detect phase changes. Section A5 discusses other shape representations.

### 2.4. Simulations

It is useful to see how the different theoretical models perform under different circumstances. In some cases, this is best done through the theoretical methods discussed above and in the Appendix especially since there are a huge number of variables that could vary in one clinical situation to another. However, simulations will allow a complementary exploration of the above ideas. In the main text some simulations are shown with more discussed in Appendix A7. All of the simulations were carried out using Mathematica (Wolfram, Champaign IL). Each evoked potential trace had 100 sample points and the base evoked potential is of the form shown in Fig. 1a (the difference between two time shifted Gaussians) and recorded signal in each trace is (0.48):

$$x(T) = \sum_{i=1}^{n} a_i s(w_i(T - \varphi_i - \tau_i)) + N(T) \tag{48}$$

where i labels each trace. The values of $\{a_i, \varphi_i, w_i\}$ are set in advance and define the particular case simulation. The noise has three components. The first is stimulus artifact and has the form $\sum_{i=1}^{n} \alpha e^{-\frac{(T-\tau_i)^2}{2\rho^2}}$ . Another component is uniformly distributed random noise over the range $[0, \delta]$ . The final noise component is sinusoidal noise of the form $\varepsilon \, \mathrm{Sin}[2\pi\rho(T - \tau_i) + \varsigma]$ . For the sake of simplicity the phase for each trace is chosen as uniformly distributed on $[-\pi, \pi]$. Each "case" consists of 100 traces. Four algorithms were studied to extract an amplitude measurement from the data. The first uses the largest peak to peak value in each trace (PP). The second uses the peak to peak amplitude values at the actual peak and trough levels expected at the peak and trough latencies in the baseline evoked potential waveform (PP-Fixed). The third uses the simple amplitude variation from the correlation receiver (0.13) (Corr Rec) and the fourth (Corr Rec+) uses a variational procedure in which different values of w (0.5–1.15 in 10 steps) and latency (−10,10 time points in steps of 1) were used to construct expected signals and the correlation receiver applied to this signal to determine amplitude. The best latencies and durations were then chosen by the parameters that provide the best fit to the recorded noisy waveform. No averaging is used and each trace is analyzed separately. This first set of simulations was performed in order to determine the ability of the methods to find the trend in evoked potential amplitude over time.

In a second set of simulations 250 repetitions of each two traces which contain evoked potentials with a 25% difference in amplitude were performed at different noise levels. This allowed a determination of the ability of different algorithms to detect 25% reduction in amplitude of the evoked response. Statistics on true and false positive detections as well as the area under the receiver operator characteristic (ROC) curve are collected for each algorithm. In addition, Cohen's D is computed as a measure of the difference between the amplitude measurements made when a = 0.75 and a = 1. The Kruskal-Wallis non-parametric test is used to compare the values of these amplitude measurements in the same two conditions.

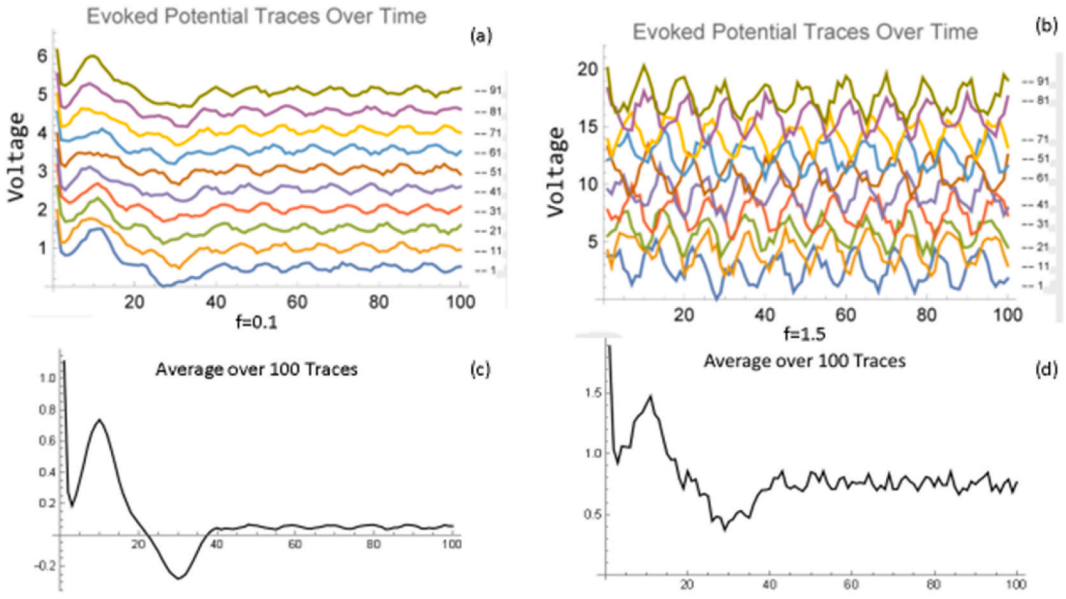


**Fig. 2.** Stack plots of some evoked potential traces during a simulated case with two different noise levels (a) f = 0.1 and (b) f = 1.5. (c) The average of the evoked potentials over 100 traces f = 0.1, (d) the average of the evoked potentials over 100 traces f = 1.5.

## 3. Results

In the first set of simulations, the amplitude of the evoked potential (0.48) recorded during the case is chosen as (0.49):

$$a_i = 1 - 2\frac{i}{100}\left(1 - \frac{i}{100}\right); \varphi_i = 0, w_i = 1;\ i = 1...100 \tag{49}$$

Thus, over a simulation comprised of 100 separate traces, the amplitude of the evoked potential signal drops by half in the middle of the simulation and returns to baseline by the end of the simulation. The signal s(t) has the form shown in Fig. 1a. This leads, in the absence of noise, to peak-to-peak amplitude changes in the actual signal shown in Fig. 1c and a stacked plot of the signal in the absence of noise for some of the traces in Fig. 1d. A typical example of the noise added to a trace is shown in Fig. 1b and has the form (0.50):

$$\varepsilon_t \sum_{i=1}^{n} e^{\frac{-(i-1)^2}{0.5}} + f[\varepsilon_w \eta_i + \varepsilon_s \ \mathrm{Sin}(0.2\pi i + \varsigma)]; \tag{50}$$

Where f (the "noise index") gives the amplitude of the noise ("log noise" in the figures refers to logf), $\eta_i$ is a uniformly distributed random variable on [0,1] (see appendix A7 for the effect of other noise choices) and is chosen independently at each sample point. $\varsigma$ is uniformly distributed on $[-\pi, \pi]$ and chosen once for each trace. $\varepsilon_t, \varepsilon_w, \varepsilon_s$ are fixed parameters determining the amplitude of the stimulus artifact, the white noise and the sinusoidal noise. Thus the noise has an initial stimulus artifact in the setting of white plus pink noise. Fig. 2a and b shows samples of some of the evoked potential traces for f = 0.1 and 1.5 respectively and Fig. 2c and d shows the averaged evoked potential over all 100 traces. For a low noise condition (f = 0.1), Fig. 3a and b shows the measured amplitude for each trace obtained using 4 different methods. They are: 1)maximum – minimum (PP) method which takes the amplitude as the difference between the maximum signal in a trace minus the minimum signal in a trace. 2) (PP-Fixed) which takes the amplitude measure as the difference between the amplitudes at the peak and trough latencies found in the baseline evoked potential. 3) (Corr Rec) is the evoked potential amplitude estimated with the correlation receiver (0.13). 4) (CorrRec+) is the amplitude measure estimated with the correlation receiver after a search over changes in latency and duration is performed to find the optimal latency and duration. In the low noise condition all yield similar results. In a high noise condition (f = 1.5), Fig. 3c shows that although there are variations in the amplitude estimated from the correlation receiver (Corr Rec), the result tracks the actual amplitude relatively well even in a case where Fig. 2b shows that there is no easily visible peak. However, Fig. 3d shows that the peak to peak methods (PP and PP-Fixed) give a very poor estimate of amplitude. Although there is a faint trend for the peak to peak amplitude measured from the baseline peak and trough latencies (PP-Fixed) to correlate with the actual changes in amplitude, it is not as clear as with the correlation receiver (Corr Rec). Note that using the corrections for changes in latency and duration (Corr Rec+) does not improve result from the simple correlation receiver as it adds to the complexity of the calculation and in the face of high noise levels increases errors (Appendix A6). This is effect of

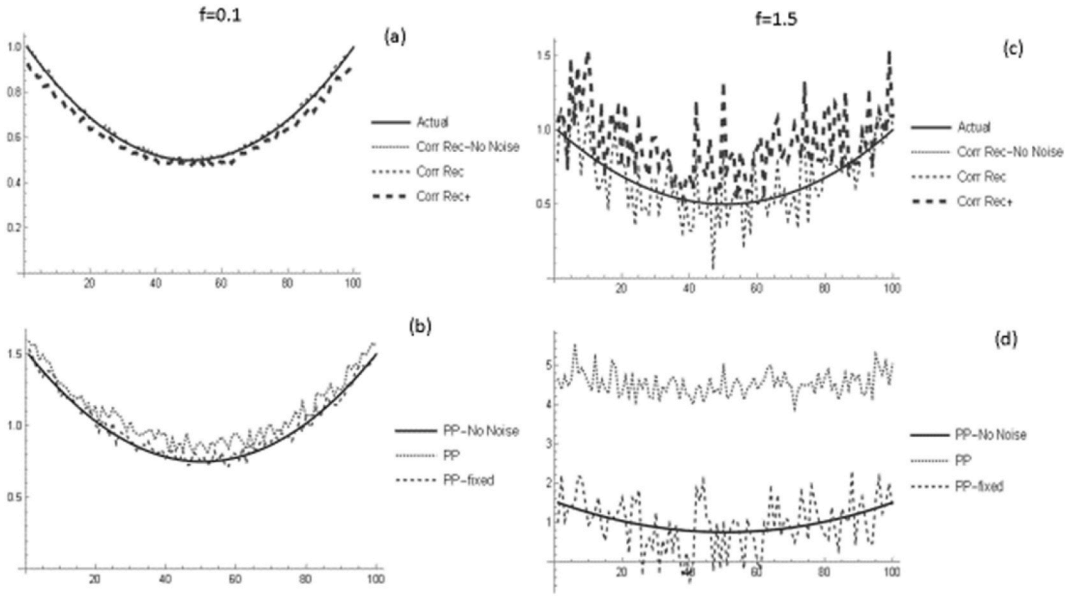


**Fig. 3.** Computed amplitude of the evoked potential using 4 methods: PP = raw peak to peak amplitude, PP-Fixed = difference between the amplitude at the points where the baseline tracing had its troughs and peaks, Corr Rec = the correlation receiver (0.28), Corr Rec+ = the correlation receiver with template matching to find optimal latency and duration shifts. (a) and (b) show the computed evoked potential amplitude compared to the actual values in the low noise condition f = 0.1. (c) and (d) show the computed evoked potential amplitude in the high noise condition f = 1.5. Although all methods give similar results in the low noise situation, only the Corr Rec method produces good results in the high noise case.

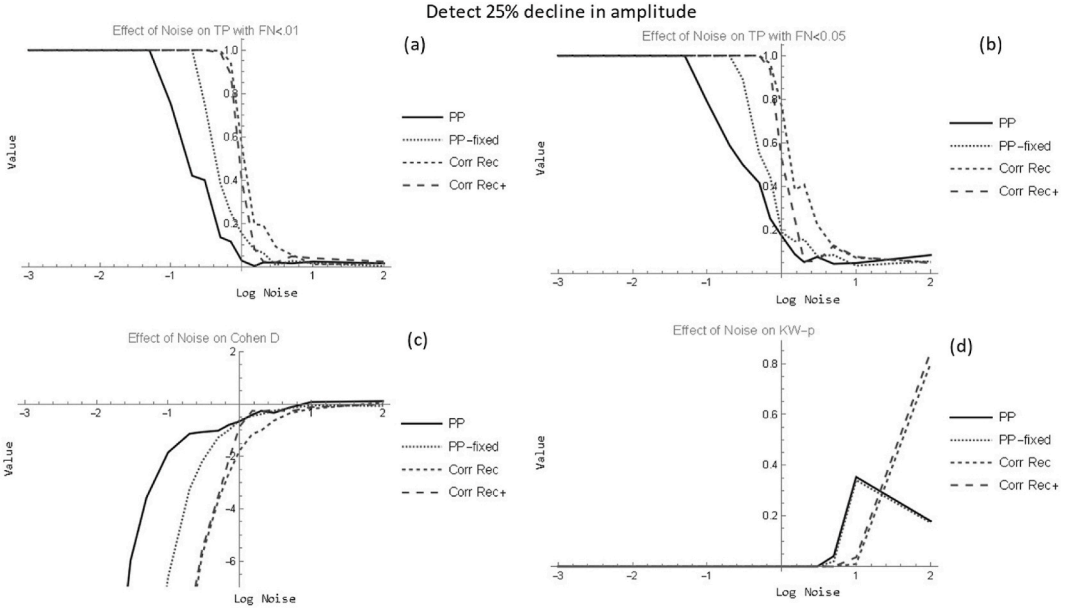


**Fig. 4.** Performance of each amplitude measure for detecting a 25% reduction in amplitude for various noise (f) values. True positive detection rate when the false negative rate is $< 0.01$ (a) and $<0.05$ (b). (c) Shows the value of Cohen's D which is a measure of the difference between the statistic values in two evoked potential traces with amplitudes of 1.0 and 0.75. Larger values indicate more significant differences. (d) The p-value generated by the Kruskal-Wallis test to see if the data in the two traces are different. All show better results with Corr Rec method which can detect signals in at least 3–5 fold more noise than the best peak to peak method.

worsening amplitude estimates in the face of fitting additional parameters is also reflected in the poorer performance of the PP as compared to the PP-Fixed methods. Figure A1 in the appendix shows the results of amplitude estimation in the case of a very high noise level $f = 5$.

Fig. 4a and c shows the ability of the various amplitude detection methods to find a difference between two evoked potential traces in which one evoked potential has a 25% lower amplitude than another, as a function of the noise level. Metrics used include the probability of a true positive detection of 25% decrease in amplitude when the false positive rate is kept less than 0.01 or 0.05 respectively. This is very high for all methods when the noise level is low but declines as the noise level increases. Overall, the best results (largest probability of a true positive detection) are seen with the correlation receiver which still allows a 50% true positive rate for $f = 1.5$ where the peak to peak methods have a value near 0.1. This same trend is also seen in the Cohen's D (Fig. 4b and d) which is larger for the correlation receiver methods than the PP methods at large noise levels indicating better detectability. Fig. 5 shows how the AUC (area under the ROC curve) changes with noise for each of the methods and is largest for the simple correlation receiver. This method has the least number of unknown variables to determine and according to the arguments in appendix A6 is likely to be associated with the lowest parameter variance estimates. Again the Corr Rec method has the largest area under the curve. The insets in Fig. 5 illustrate the actual ROC curves for the (PP) and (Corr Rec) methods when the noise amplitude is unity. Figure A2 in the appendix shows that the ROC curves for each method in the low and high noise conditions. Figure A15 illustrates this again at different values of the noise.

Other simulations in which the effects of the different types of noise, the shape of the evoked potential and the shape of the template are explored are shown Appendix A7.

## 4. Discussion

This paper has investigated methods to extract amplitude and shape information from evoked potentials obtained during IONM. This is a unique problem because the presence of a pre-surgical baseline allows for the use of pattern matching to the responses recorded in real time. In this case, the correlation receiver can provide a more reliable estimate of the evoked potential amplitude than measuring the peak to peak amplitude when the evoked potential is embedded in noise. Qualitatively, the correlation receiver reduces the effect of noise by averaging over the noise **within** an individual response since the form of the evoked potential is known. The traditional approach in clinical evoked potentials of averaging results from sequential traces is the optimal approach only when the responses are known to be stable from trial to trial and there is no a priori information about the expected response. In many ways the correlation receiver concept which involves matching patterns more closely mimics the process of visual analysis than that of simple averaging. Averaging and the correlation receiver are not exclusive techniques and in the steady state can be combined to provide even better evoked potential estimates than either method alone. It is important to note that reasonable estimates of amplitude trends may

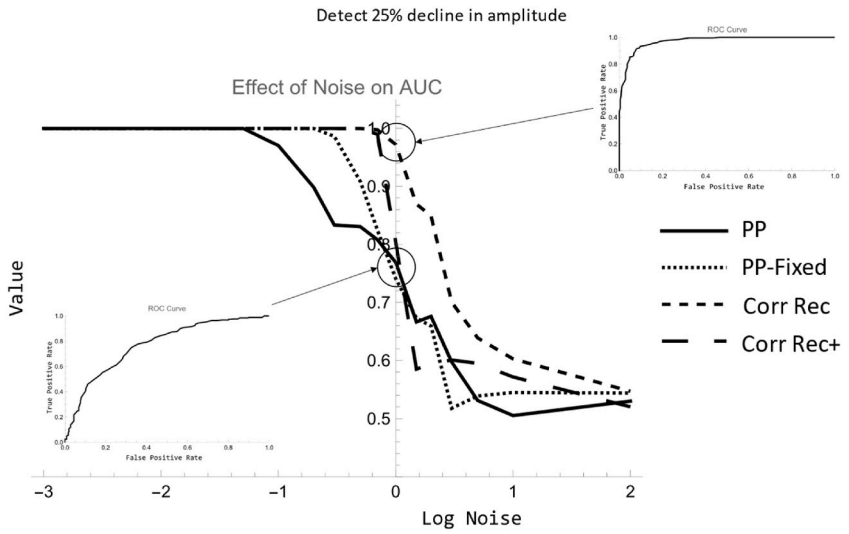


**Fig. 5.** The area (AUC) under the receiver operating characteristic (ROC) curve for each of the amplitude detection methods as a function of noise level to find differences between two traces in which the amplitude of the ep is different by 25%. The Corr Rec method clearly outperforms the other methods with a larger AUC indicating a better ability to discriminate between the two traces. At the bottom right the ROC curve for the PP method is shown for log noise = 0. At the upper right the ROC curve for the Corr Rec method is shown for log noise = 0.

result even if the trial function is somewhat different from the actual evoked potential (2.3.2, A3, A7).

One important observation is that the variance of the correlation receiver amplitude estimates depends on the correlation time of the noise. The shorter the noise correlation time (i.e. closer to white noise) the better the amplitude estimate. Thus, increasing the sampling rate to fully define the noise will prevent a falsely high correlation time that could arise from under sampled noise and will improve the amplitude estimates. Increasing the sample rate within the traditional averaging framework would not be helpfulwhere no information about the evoked potential is assumed. As per equation (0.30) the effect of linear transformations or filtering the data do not change the amplitude estimates in the absence of noise. In the setting of zero mean noise, although the mean amplitude is unchanged by these transformations, the variance of the estimates may be difficult to estimate. Thus, some a priori investigations of these

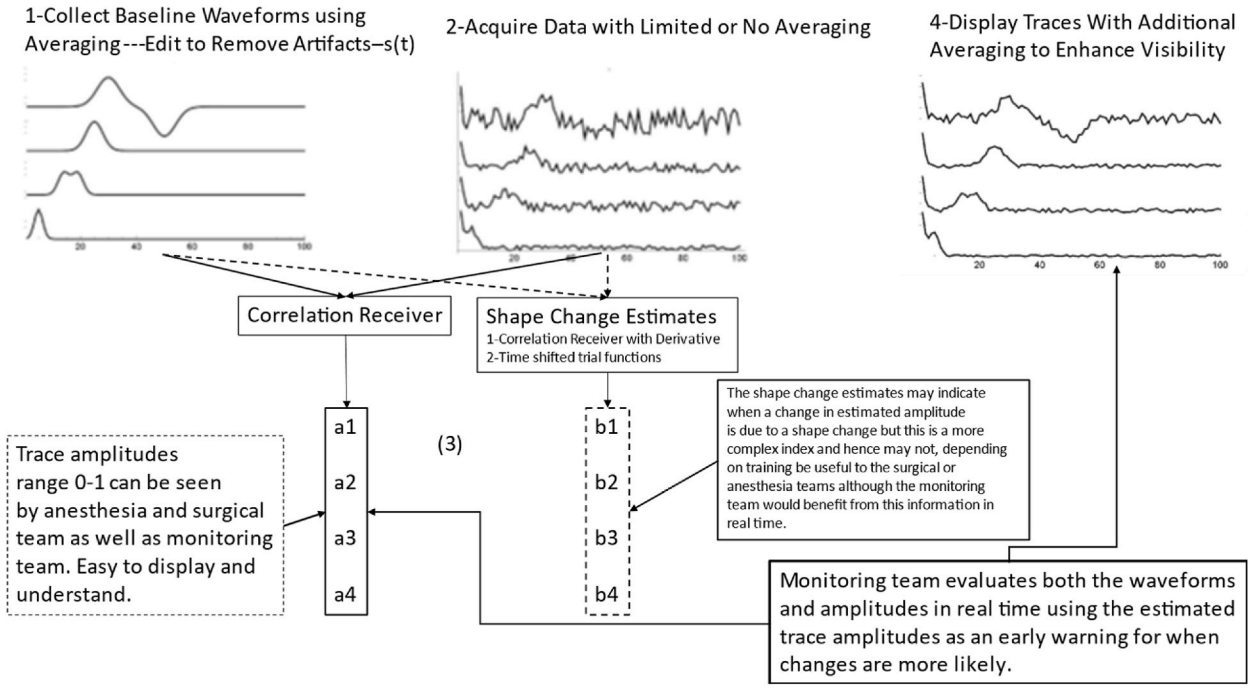


**Fig. 6.** Illustration as to how to incorporate the amplitude measures during intra-operative neurophysiologic monitoring.

effects before using data transformations in a clinical situation.

Methods for extracting information on changes in the shape of the evoked potential waveform were also explored. Direct estimates of changes in latency could be made by shifting the recorded waveform and finding the time shift required to optimize the match to the baseline potential but in the presence of noise this adds uncertainty to the amplitude estimate. Applying the correlation receiver with the derivative of the baseline potential gives zero when the shape of the current waveform is the same as that of the baseline and deviations from zero are proportional to the time lag and so this provides a simple method of assessing shape changes. Other methods were explored but this is a simple method to highlight when there may be significant shape changes (A5).

This leads us to propose the following process for monitoring evoked potentials during surgery (Fig. 6):

1 -Use averaging and clinical intuition to define the expected baseline evoked response $s(t)$ for each monitored channel.
2 -Apply the simple correlation receiver to data with the minimum number of averages needed. At the same time compute the result of the correlation receiver with the s'(t) as a measure of the change in shape (potentially other indices may be valuable as in Appendix A5). The number of averages to provide good estimates for the shape changes may be different than the number to get a good amplitude estimate but this can be chosen during the recording session.
3 -Display the relative amplitudes (and shape change markers) prominently so that not only the monitoring team but the surgical team and anesthesia teams can see them. These values are simple to interpret and as such are better understood by non-neurophysiologists than raw evoked potential waveforms.
4 -The monitoring team reviews both these values and the waveforms obtained with the traditional averaging techniques and generates alerts when appropriate.
5 -When possible, continuously compare the lowest amplitudes in relevant channels to previously recorded data to estimate the probability of a neurologic deficit (This includes the effects of all measures to remediate changes by the local surgical, anesthesia and monitoring teams.). See appendix A4.

## Author contribution statement

Mark Menniti Stecker: Conceived and designed the experiments; Performed the experiments; Analyzed and interpreted the data; Contributed reagents, materials, analysis tools or data; Wrote the paper. Jonathan Wermelinger, Jay Shils: Analyzed and interpreted the data; Wrote the paper.

## Data availability statement

Data will be made available on request.

## Declaration of competing interest

The authors declare the following financial interests/personal relationships which may be considered as potential competing interests:M.S. is president of the Fresno Institute of NeuroscienceJ.S. is a consultant with Inomed and is on the board of directors of NervioJ.W. has nothing to declare.

## Appendix A. Supplementary data

Supplementary data to this article can be found online at https://doi.org/10.1016/j.heliyon.2023.e18671.

## References

[1] A. Moller, Chapter 17. General considerations, in: A. Moller (Ed.), Intraoperative Neurophysiologic Monitoring, second ed., Humana Press, Totawa, NJ, 2006, pp. 283–297.
[2] M. Stecker, T. Patterson, Electrode impedance in neurophysiologic recordings 2. Role in electromagnetic interference, Am J END Tech 39 (1999) 34–51.
[3] M.M. Stecker, T. Patterson, Electrode impedance in neurophysiologic recordings: 3.Effects on recorded signals, Am J END Technol 39 (1999) 148–164.
[4] M. Stecker, T. Patterson, Electrode impedance in neurophysiologic recordings 1. Theory and intrinsic contributions to noise, Am J END Tech 38 (1998) 174–198.
[5] M.M. Stecker, T. Patterson, Strategies for minimizing 60 Hz pickup during evoked potential recording, Electroencephalogr. Clin. Neurophysiol. 100 (4) (1996) 370–373.
[6] M.M. Stecker, Generalized averaging and noise levels in evoked responses, Comput. Biol. Med. 30 (5) (2000) 247–265.
[7] M.V. Spreckelsen, B. Bromm, Estimation of single-evoked cerebral potentials by means of parametric modeling and Kalman filtering, IEEE (Inst. Electr. Electron. Eng.) Trans. Biomed. Eng. 35 (1988) 691–700.
[8] D.B. MacDonald, C. Dong, R. Quatrale, F. Sala, S. Skinner, F. Soto, et al., Recommendations of the international society of intraoperative neurophysiology for intraoperative somatosensory evoked potentials, Clin. Neurophysiol. 130 (1) (2019) 161–179.
[9] R.N. McDonough, A.D. Whalen, Detection of Signals in Noise, Academic Press, New York, New York, 1995.
[10] G.C. Carter (Ed.), Coherence and Time Delay Estimation, IEEE Press, New York, New York, 1993.
[11] D.H. Lange, H. Pratt, G.F. Inbar, Modeling and estimation of single evoked brain potential components, IEEE Trans. Biomed. Eng. 44 (9) (1997) 791–799.
[12] C.D. McGillem, J.I. Aunon, K.B. Yu, Signals and noise in evoked brain potentials, IEEE Trans. Biomed. Eng. 32 (12) (1985) 1012–1016.
[13] N. Yu, Y. Chen, L. Wu, H. Lu, Single-trial evoked potential estimating based on sparse coding under impulsive noise environment, J. Pharm. Pharmacol. 3 (2015) 556–561.

[14] P. Ungan, E. Basar, Comparison of Wiener filtering and selective averaging of evoked potentials, Electroencephalogr. Clin. Neurophysiol. 40 (5) (1976) 516–520.
[15] D.J. Doyle, A proposed methodology for evaluation of the Wiener filtering method of evoked potential estimation, Electroencephalogr. Clin. Neurophysiol. 43 (5) (1977) 749–751.
[16] Y. Song, C.S. Lindquist, Summary of time-frequency algorithms for processing auditory evoked potentials, in: Conference Record of Thirty-Fifth Asilomar Conference on Signals, Systems and Computers 1, 2001, pp. 829–833. Cat.No.01CH37256.
[17] N. Yu, L. Wu, D. Zou, Y. Chen, H. Lu, A MISO-ARX-based method for single-trial evoked potential extraction, BioMed Res. Int. 2017 (2017), 7395385.
[18] Palaniappan R. , Anandan S, and Raveendran P. Two level PCA to reduce noise and EEG from evoked potential signals, in: 7th International Conference on Control, Automation, Robotics and Vision, 1688-1693 vol.3 2002. ICARCV 2002.;.
[19] Cichocki A., Gharieb R. R., and Hoya T. Efficient extraction of evoked potentials by combination of Wiener filtering and subspace methods. - 2001 IEEE International Conference on Acoustics, Speech, and Signal Processing. Proceedings3117-3120 vol.5 (2001) Cat. No.01CH37221.
[20] R.J. Bufacchi, C. Magri, G. Novembre, G.D. Iannetti, Local spatial analysis: an easy-to-use adaptive spatial EEG filter, J. Neurophysiol. 125 (2) (2021) 509–521.
[21] A. LeBron Paige, O. Ozdamar, R.E. Delgado, Two-dimensional spectral processing of sequential evoked potentials, Med. Biol. Eng. Comput. 34 (3) (1996) 239–243.
[22] Strauss D.J. Teuber T., Steidl G., Corona-Strauss F.I. Exploiting the Self-Similarity in ERP Images by Nonlocal Means for Single-Trial Denoising. IEEE Trans. Neural Syst. Rehabil. Eng. 21 (4) (2013) 576–583.
[23] P. Bansal, M. Sun, R.J. Sclabassi, Simulation and extraction of single-trial evoked potentials, Conf Proc IEEE Eng Med Biol Soc 2006 (2004) 200–203.
[24] K. Chiappa, Evoked Potentials in Clinical Medicine, Lippincott-Raven Publishers, Philadelphia, 1997.
[25] M.H. Cuypers, J.M. Thijssen, Improving the ensemble average of visual evoked potentials. II. Simulations and experiments, Technol. Health Care 3 (1) (1995) 33–42.
[26] J.M. Thijssen, M.H. Cuypers, Improving the ensemble average of visual evoked potentials. I. Theory of correction by spectral phase difference methods, Technol. Health Care 3 (1) (1995) 23–31.
[27] D. Liberati, S. Cerutti, E. Di Ponzio, V. Ventimiglia, L. Zaninelli, The implementation of an autoregressive model with exogenous input in a single sweep visual evoked potential analysis, J. Biomed. Eng. 11 (4) (1989) 285–292.